Requirements for endoderm and BMP signaling in sensory neurogenesis in zebrafish

Jochen Holzschuh[1,*], Naoyuki Wada[1], Chikako Wada[1], Ashleigh Schaffer[1], Yashar Javidan[1], Alexandra Tallafuß[2,3,†], Laure Bally-Cuif[2,3] and Thomas F. Schilling[1,‡]

[1]Department of Developmental and Cell Biology, University of California, 5438 McGaugh Hall, Irvine, CA 92697-2300, USA
[2]Zebrafish Neurogenetics Junior Research Group, Institute of Virology, Technical University-Munich, Trogerstrasse 4b, D-81675 Munich, Germany
[3]GSF-National Research Center for Environment and Health, Institute of Developmental Genetics, Ingolstaedter Landstrasse 1, D-85764 Neuherberg, Germany

*Present address: Department of Developmental Biology, University of Freiburg, Biology I, Hauptstrasse 1, 79104 Freiburg, Germany
†Present address: Institute of Neuroscience, 1254 University of Oregon, Eugene, OR 97403-1254, USA
‡Author for correspondence (e-mail: tschilli@uci.edu)

Accepted 13 June 2005

Development 132, 3731-3742
Published by The Company of Biologists 2005
doi:10.1242/dev.01936

Summary

Cranial sensory neurons largely derive from neurogenic placodes (epibranchial and dorsolateral), which are ectodermal thickenings that form the sensory ganglia associated with cranial nerves, but the molecular mechanisms of placodal development are unclear. Here, we show that the pharyngeal endoderm induces epibranchial neurogenesis in zebrafish, and that BMP signaling plays a crucial role in this process. Using a *her5:egfp* transgenic line to follow endodermal movements in living embryos, we show that contact between pharyngeal pouches and the surface ectoderm coincides with the onset of neurogenesis in epibranchial placodes. By genetic ablation and reintroduction of endoderm by cell transplantation, we show that these contacts promote neurogenesis. Using a genetic interference approach we further identify *bmp2b* and *bmp5* as crucial components of the endodermal signals that induce epibranchial neurogenesis. Dorsolateral placodes (trigeminal, auditory, vestibular, lateral line) develop independently of the endoderm and BMP signaling, suggesting that these two sets of placodes are under separate genetic control. Our results show that the endoderm regulates the differentiation of cranial sensory ganglia, which coordinates the cranial nerves with the segments that they innervate.

Key words: Epibranchial, Placode, Zebrafish, Neural crest, Endoderm, Pharyngeal arches, Pharyngeal pouches, BMP, Segmentation

Introduction

Development of the peripheral nervous system involves the coordinated development of two uniquely vertebrate cell types, placodes and neural crest. During head development, focal thickenings of ectoderm called neurogenic placodes give rise to neurons in the paired sense organs and cranial sensory ganglia associated with cranial nerves (LeDouarin, 1982; Graham and Begbie, 2000; Baker and Bronner-Fraser, 2001). These are joined by neurogenic neural crest cells to generate the mature ganglia. Some neurogenic placodes develop close to the neural tube, whereas others form next to segmented outpockets of the endoderm called 'pouches' that bud from the lateral walls of the pharynx, which may play important roles in placodal induction and neurogenesis (Goodrich, 1930). There is growing evidence to suggest that, despite their similar appearance, each placode is induced by a different combination of signals from the surrounding tissues (Baker and Bronner-Fraser, 2001).

Neurogenic placodes can be split into two groups, dorsolateral (trigeminal and vestibular) and epibranchial (including the facial or geniculate, VII; glossopharyngeal or petrosal, IX; vagal or nodose, X), which innervate taste buds, the heart and other visceral organs. Neural progenitors within the placodes are first specified by the expression of the basic helix-loop-helix (bHLH) transcription factors *neurogenin 1* (*ngn1*; *neurog1* – Zebrafish Information Network), *neurogenin 2* (*ngn2*; *neurog3* – Zebrafish Information Network) and *neurod* (Sommer et al., 1996; Anderson, 1999; Andermann et al., 2002; Begbie et al., 2002). Distinct subsets of placodes express these factors in different species (Schlosser and Northcutt, 2000), and each is required at an early stage in the specification of neural progenitors. Targeted inactivation of *Ngn2* specifically disrupts epibranchials (Fode et al., 1998), while *Ngn1* is required in dorsolateral placodes in mice (Ma et al., 1998), and in all neurogenic placodes in zebrafish (Andermann et al., 2002), further suggesting that separate mechanisms control dorsolateral and epibranchial development. The paired homeodomain transcription factors *Phox2a* and *Phox2b* are also required for epibranchial differentiation and survival (Tiveron et al., 1996; Valarche et al., 1993). Thus placodes are distinguished by unique patterns of neurogenesis, and these may reflect their responses to different signals.

Pharyngeal pouches in the endoderm are thought to induce

neurogenesis in the epibranchial placodes through expression of bone morphogenetic protein 7 (BMP7), a member of the transforming growth factor beta (TGFβ) superfamily (Begbie et al., 1999; Luo et al., 1995). Both endoderm and exogenous BMP7 protein can induce neural progenitors in ectodermal explants in culture. Once epibranchial sensory neurons have established their axonal connections, their survival depends upon glial-derived neurotrophic factor (GDNF), which is also a member of the TGFβ superfamily (Buj-Bello et al., 1995). By contrast, a signal from the prospective midbrain-hindbrain boundary (MHB), possibly a fibroblast growth factor (FGF) is thought to induce the trigeminal (Stark et al., 1997; Baker et al., 1999), and the otic placode depends on FGF signaling from the hindbrain (Phillips et al., 2001). These studies suggest that epibranchial and dorsolateral placodes are induced by different signals depending on their proximity to the endoderm or neural tube.

Pharyngeal endoderm also physically interacts with neural crest mesenchyme that forms cartilage and bone, and promotes skeletal differentiation (Hall, 1980; Le Douarin, 1982). Recent evidence suggests that, in this context, the endoderm plays an instructive role in anteroposterior (AP) patterning, as removing and reinserting the pharyngeal endoderm in a reversed AP orientation can cause mandibular duplications (Couly et al., 2002). Zebrafish *casanova* (*cas*; *sox32* – Zebrafish Information Network) (Kikuchi et al., 2000; Dickmeis et al., 2001) mutants, which lack all endoderm, fail to form pharyngeal cartilages due to a lack of local cartilage-inducing signals (David et al., 2002). The pharyngeal pouches appear to play a crucial role in this interaction, because in *van gogh* (*vgo*; *tbx1* – Zebrafish Information Network) mutants, as well as mutants that lack *integrin alpha 5* function, defects in pouch formation correlate with subsequent cartilage malformations (Piotrowski and Nusslein-Volhard, 2000; Piotrowski et al., 2003; Crump et al., 2004a). The primary defect in all of these cases lies in the endoderm, as reintroduction of endodermal cells into mutants rescues cartilage formation and pharyngeal patterning.

Here, we report that the pharyngeal endoderm is required for the induction of the epibranchial nervous system in zebrafish, and that BMPs play an important role in this process. The sequential formation of pharyngeal pouches correlates precisely with the onset of neurogenesis in the epibranchial placodes, which we show by following endodermal morphogenesis in the living embryo. Mutants that disrupt pouch formation, such as *cas* and *vgo*, have corresponding defects in epibranchial, but not dorsolateral, placodes. We further show that the reintroduction of wild-type endoderm can rescue epibranchial development in *cas* mutants. Several lines of evidence suggest that this interaction depends on BMP signaling, including endoderm-specific inhibition of BMPs, as well as exogenous application of BMP proteins or BMP inhibitors. These are the first studies to show that the endoderm is required to induce neurogenesis in epibranchial placodes (but not dorsolateral placodes) in vivo, and that BMPs other than BMP7 are involved. In addition, they go beyond previous work in demonstrating that endodermal segmentation (pouch formation) controls the spatial patterning of sensory neurogenesis in the embryo.

Materials and methods

Animals

Embryos were produced by paired matings of zebrafish (*Danio rerio*), and staged in hours post-fertilization (hpf), as described previously (Kimmel et al., 1995; Westerfield, 1995). Embryos homozygous for the *casanova* (*cas*^{ta56}), *van gogh* (*vgo*^{tm208}) and *snailhouse* (*snh*^{ty68}) mutations were derived from matings between heterozygous carriers, and scored by their heart, ear or tail defects, respectively (Kikuchi et al., 2000; Dickmeis et al., 2001; Piotrowski et al., 1996; Dick et al., 2000).

Transgenics

A fragment containing 700 bp of *her5* upstream sequence driving *egfp* (*–0.7her5:egfp*) was obtained by PCR from a larger construct containing 3650 bp (*her5PAC:egfp*), as described previously (Tallafuss and Bally-Cuif, 2003). This was purified and injected as a linear fragment into fertilized eggs at the one-cell stage at a concentration of 50 ng/μl. Embryos were then raised to adulthood and mated with wild-type adults. F1 embryos expressing *egfp* were identified and mated with wild types to establish the transgenic lines. Homozygous *her5:egfp* transgenic fish were then generated in natural matings, and expression verified over at least three generations.

Confocal imaging

For analysis of pouch formation, pharyngeal endoderm was labeled by the *her5:egfp* transgene starting at 14-15 hpf. Transgenic embryos were manually dechorionated and anesthetized with ethyl-m-aminobenzoate methane sulfanate (Westerfield, 1995), transferred to 0.5% agarose in embryo medium and then mounted on a coverslip. Approximately 80 μm Z-stacks at 6 μm intervals were captured using a Zeiss LSM510 Meta confocal fluorescence microscope.

Cell transplantation

Cell transplantations were targeted to the endoderm using either an injection of mRNA encoding the activated Taram-A receptor (tar*), as previously described (Aoki et al., 2002a; Aoki et al., 2002b; David et al., 2002), or *cas* (*sox32*) mRNA (Dickmeis et al., 2001). Briefly, wild-type donor embryos were injected at the one-cell stage with a mixture of 2% tetramethylrhodamine-isothiocyanate dextran and 3% lysine-fixable biotin dextran (10,000 M_r, Molecular Probes) together with 1 ng *cas* or 1 pg tar* RNA (*cas*/dextran or tar*/dextran, respectively). At late blastula stages, cells from these RNA-injected donors were transplanted to the margins of wild-type or *cas* mutant hosts. The resulting mosaic embryos were selected using a Leica fluorescence stereomicroscope for those containing large numbers of transplanted cells in the pharyngeal endoderm. Such transplants were typically restricted to one side of the pharynx or to individual pouches, with the contralateral side serving as a control and allowing the identification of rescued *cas* mutants.

Morpholino studies

Morpholino oligomers targeted to the translation start sites of *bmp2b*, *bmp7* (Imai and Talbot, 2002) and *bmp5* (GenBank #NM 201051 – CCACAGAAGTTCCAAATGTTCTCAT) were obtained from Gene Tools, diluted in 1×Danieau's buffer and injected together with the tar*/dextran or *cas*/dextran mixtures. Volumes injected were calculated for each microinjection needle at a particular injection pressure, using a micrometer imprinted on a glass slide to measure the diameter of a droplet produced at its tip with a single injection pulse. Amounts injected per embryo were then chosen for each morpholino that phenocopied loss-of-function mutations: 300 pg of *bmp2b* MO phenocopies *swirl* mutants; 900 pg of *bmp7* MO phenocopies *snailhouse* mutants (Imai and Talbot, 2002). For *bmp5*, we found that 1 ng of the *bmp5*-MO caused a slight reduction in head size, but otherwise no clear phenotype on its own, but effectively reduced epibranchials when injected into endoderm. A similar result was obtained using a second, non-overlapping *bmp5*-MO.

Bead implantation

Human recombinant BMP4, BMP5, BMP7 and Noggin proteins (R&D Systems) were used for bead implantation experiments. CM-Affi-Gel Blue beads (diameter: 70-100 μm, Bio-Rad) were incubated in each protein solution (BMPs, 1-10 μg/ml; NOGGIN, 100-500 μg/ml) at 4°C for 1 hour. Using a tungsten needle, a small slit was made anterior to the otic vesicle on one side of the head at 20 hpf. A protein-coated bead was inserted into the hole, and positioned beneath the ectoderm. Embryos were raised to 48 hpf, and fixed for *phox2b* analysis by in situ hybridization. As controls, we used beads coated in 1% BSA-PBS.

Histology

In situ hybridization was carried out as described previously (Thisse et al., 1993). Probes used were: *bmp2a*, *bmp2b* and *bmp4* (Martinez-Barbera et al., 1997), *bmp7* (Dick et al., 2000), *neurod* (Korzh et al., 1998), *foxi1* (Nissen et al., 2003; Solomon et al., 2003) and *phox2a* (Guo et al., 1999). A cDNA encoding *bmp5* was isolated from a gridded zebrafish pharyngula-stage (24 hpf) library using human BMP7 as a probe, cloned into the pSPORT vector. To generate a *bmp5* probe for in situ hybridization, we linearized with *Eco*RI and transcribed with SP6. To generate a probe specific for *phox2b* expression, we amplified by RT-PCR the complete coding sequence of zebrafish *phox2b* (GenBank #AY166856), using primers designed from *phox2b* genomic sequence (Sanger Centre, Hinxton, UK). The PCR product was cloned into the pBS-KS vector and verified by sequencing. To generate the probe containing the *phox2b* complete coding sequence, we linearized with *Kpn*1 and transcribed with T3 polymerase.

Immunolabeling with the anti-Hu and Zn-8 antibodies was done as described previously (Marusich et al., 1994; Trevarrow et al., 1990). After incubation in the primary antibodies, embryos were incubated with biotin-conjugated secondary antibodies using the Vectastain Kit, following the manufacturers instructions. For double staining, standard in situ hybridization was followed by three washes for 5 minutes each in 0.1 M glycine buffer (pH 2) before proceeding with immunohistochemistry.

For sectioning, embryos labeled by in situ hybridization or immunohistochemistry were embedded in 1 ml of gelatin-albumin (0.025 g gelatin, 1.3 g BSA, 0.9 g saccharose, in 4.5 ml PBS) for 1 hour at room temperature. This mixture was then replaced with 1 ml of gelatine-albumin + 35 μl of 50% gluteraldehyde. The embedding mixture was allowed to harden overnight at 4°C. Sections were cut at 10-20 μm with a vibratome (VT1000S, Leica), and mounted in Glyergel (Dako).

Results

Heterogeneity within the epibranchial ganglia

Epibranchial placodes in the zebrafish first express the bHLH genes *ngn1* and *neurod* beginning at 24 hpf in three cell clusters (facial, glossopharyngeal and vagal) (Andermann et al., 2002). At 30 hpf, some neuroblasts within the placodes express *phox2b* and become immunoreactive for anti-Hu (α-Hu) antibody (Fig. 1A,B) (Raible and Kruse, 2000). By 48 hpf, all six epibranchial ganglia have formed and enlarged dramatically (Fig. 1C,D). To examine the sequence of neuronal maturation in these ganglia more precisely, we performed double staining with in situ hybridization for *neurod* or *phox2b* combined with anti-Hu immunohistochemistry. We found that although *neurod* and Hu are co-expressed in dorsolateral placodes (trigeminal, auditory, vestibular, lateral line; Fig. 1A), they only partially overlap in the emerging glossopharyngeal/petrosal (gIX) and vagal/nodose (gX_{1-4}) ganglia. Distal cells within each ganglion express *neurod*,

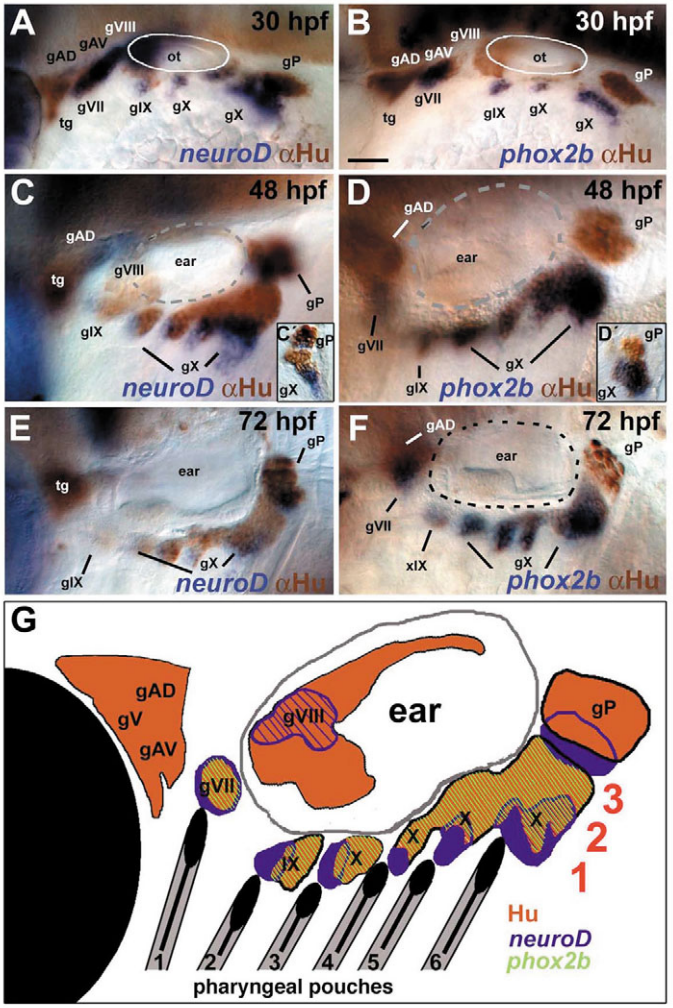

Fig. 1. Molecular markers of neurogenesis reveal heterogeneity within the epibranchial ganglia. Lateral views, anterior to the left, showing the pattern of dorsolateral and epibranchial ganglia at 30 (A,B), 48 (C,D) and 72 (E,F) hpf. Insets show vibratome sections of epibranchial ganglia from *neurod*/α-Hu (C′) and *phox2b*/α-Hu (D′) double-stained 48 hpf embryos. (A,C,C′,E) In situ hybridization to detect *neurod* mRNA in newly specified neural progenitors (blue), partially overlaps with α-Hu staining in differentiating neurons (brown). (B,D,D′,F) Most neural progenitors co-express *phox2b* at 30 hpf (B) but expression becomes restricted to a more proximal populations by 48 and 72 hpf (D,F). (G) Diagram indicating the spatial relationships of pharyngeal pouches (1-6, black), and three domains of gene expression within the ganglia (1-3, red). Hu+ proximal neural progenitors are shown in orange, *phox2b*+ cells in green (overlap with Hu is indicated as diagonal hatching) and more distal *neurod*+ cells in blue. gAD, dorsal anterior lateral line; gAV, ventral anterior lateral line; gP, posterior lateral line; gV, trigeminal; gVII, facial (geniculate), gVIII, auditory; gIX, glossopharyngeal (petrosal); gX, vagal (nodose); ot, otic placode; tg, trigeminal. Scale bar: 50 μm.

whereas more proximal cells express Hu, and this pattern persists at 48 and 72 hpf, suggesting that neuroblasts are generated distally and become displaced proximally as they mature (Fig. 1C,C′,E). Consistent with this hypothesis, *phox2b* mRNA and Hu antigen co-localize in proximal cells in each epibranchial ganglion (Fig. 1D,D′,F). Based on these studies,

we can define three distinct cell populations within an epibranchial ganglion in a distal to proximal order: (1) distal cells expressing *neurod* alone; (2) intermediate cells expressing Hu antigen, *phox2a*, *phox2b* and *neurod*; and (3) proximal cells expressing Hu, *phox2a* and *phox2b*, but not *neurod*. Thus, newly generated *neurod*+ neural progenitors are born directly adjacent to the dorsal ends of the pharyngeal pouches, and then downregulate *neurod* and express *phox2b* as they mature within the ganglion and are displaced proximally (Fig. 1G). Labeling of placodal cells in the chick has demonstrated a similar proximal displacement (Begbie and Graham, 2001).

Correlating pouch formation and placode specification with *her5*:*egfp*

The initiation of epibranchial neurogenesis around 24 hpf roughly coincides with the time at which the pharyngeal endoderm segments into pouches in zebrafish (Crump et al., 2004b). To correlate these two sets of events more precisely and to better understand the cellular basis of pharyngeal segmentation, we made time-lapse recordings of endodermal development using a transgenic line in which 700 bp of the *her5* promoter drive *egfp* expression in the pharynx. *her5* is the earliest known selective marker of pharyngeal cells (Bally-Cuif et al., 2000), and this –0.7*her5:egfp* transgene (hereafter referred to as *her5:egfp*) faithfully reproduces expression in the pharyngeal endoderm beginning at 13-14 hpf, with minimal expression in the nervous system (Fig. 2A) (Tallafuss and Bally-Cuif, 2003). Expression persists in the forming pouches and medial endoderm (Fig. 2B,D). Confocal imaging of *her5*:*egfp* expression between 15-36 hpf revealed that lateral endodermal cells become elongated mediolaterally (16-18 hpf) to form the primordia of the first and second pouches (Fig. 2C). These primordia consist of groups of six to ten cells in which the most lateral cells extend filopodial extensions to contact the surface ectoderm (arrow in Fig. 2E,F). *her5:egfp* also marks continuous bands of more medial endodermal cells that connect two adjacent pouches along the AP axis, which surround the unlabeled mesenchyme of each pharyngeal arch. The first two pouches contact the ectoderm almost simultaneously between 20 and 22 hpf (Fig. 2E,F), the third and fourth pouches at 24 and 28 hpf, respectively (Fig. 2G), while the remaining pouches (5-6) form at roughly 3 hour intervals thereafter (Fig. 2I).

To correlate the time at which a pouch contacts the ectoderm more directly with the specification of neural progenitors in the adjacent placode, pouches were imaged with confocal microscopy in individual *her5*:*egfp* transgenic embryos, and then immediately fixed and analyzed for *neurod* expression by in situ hybridization (Fig. 2H,J). In most cases (17/20) the number of *neurod*+ ganglia closely matched the number of fully formed pouches. This suggests that neurogenesis in the ectoderm occurs within a few hours of endodermal contact, consistent with a direct interaction.

Defects in epibranchial development in endodermal mutants

Pharyngeal endoderm promotes neurogenesis in ectodermal explants (Begbie et al., 1999) but whether or not it is required in vivo remains unclear. Thus, we examined markers of epibranchial neurons in *casanova* (*cas*, *sox23*) and *van gogh* (*vgo*, *tbx1*) mutants, which are defective in endoderm. *cas* mutants lack all endoderm at 48 hpf, including the pharyngeal endoderm, as shown by immunolabeling with the zn-8 antibody, which recognizes DM-GRASP (Fig. 3A,B). To determine whether epibranchial sensory neurons differentiate in the absence of endoderm we used the α-Hu antibody. *cas* mutants also lack virtually the entire epibranchial nervous system at 48 hpf, including gVII, gIX and the distal portions of gX_{1-4} (Fig. 3C,D). Consistent with a defect in placodal neurogenesis,

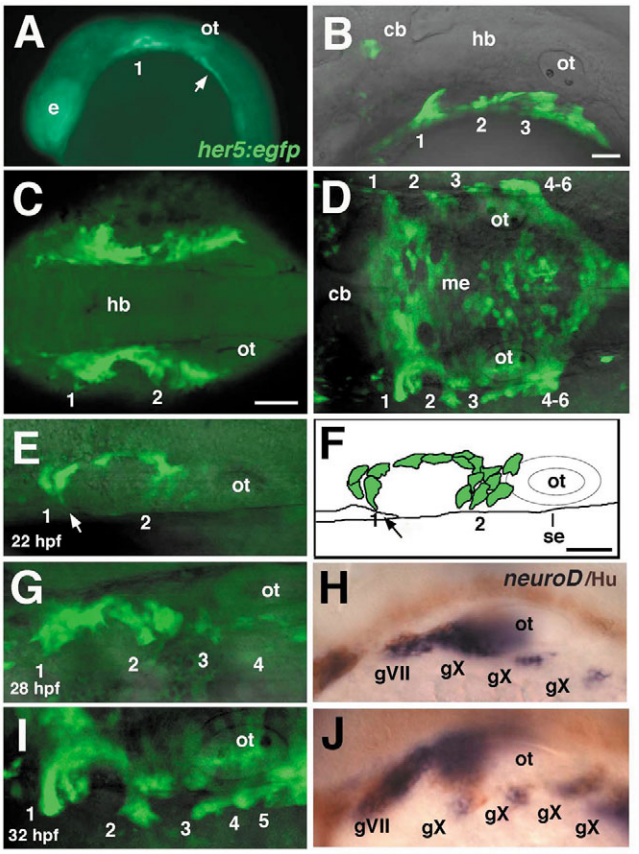

Fig. 2. Pharyngeal pouch formation coincides with epibranchial neurogenesis. (A-E,G,I) Confocal images of live, homozygous *her5:egfp* transgenic embryos; anterior to the left. (A) 16 hpf embryo, lateral view; pouch 1, as well as an unsegmented endoderm located further posteriorly (arrow), is labeled. (B) 26 hpf embryo, lateral view; pouches 1-3 are labeled. (C) 18 hpf embryo, dorsal view; pouches 1 and 2 on each side are joined along the AP axis by a continuous band of endoderm surrounding mesenchyme of the second arch. (D) 32 hpf embryo, dorsal view; pouches (1-6) form only in the most lateral endoderm, while *her5:egfp* also labels a flattened layer of medial endoderm (me). (E,G,I) Sequence of confocal images of *her5:egfp*, in dorsal view, at 22 (E), 28 (F) and 32 (H) hpf. (E) 22 hpf embryo; pouch-forming endodermal cells extend filopodial processes laterally (arrow). (F) An illustration of the embryo shown in E. Arrow indicates movement of GFP+ cells toward the surface ectoderm (se). (G-J) Embryos analyzed for *her5:egfp* expression at 28 (G) and 32 (I) hpf were fixed and subjected to in situ hybridization (H,J) for *neurod* (blue) combined with immunolabeling with α-Hu antibody (brown). 1-6, pharyngeal pouches; cb, cerebellum; e, eye; gV, trigeminal ganglion; gVII, facial (geniculate) ganglion; gIX, glossopharyngeal (petrosal) ganglion; gX, vagal (nodose) ganglion; hb, hindbrain; me, medial endoderm; ot, otic vesicle. Scale bars: 50 μm; in B for A,B; in C for C,D; in F for E-J.

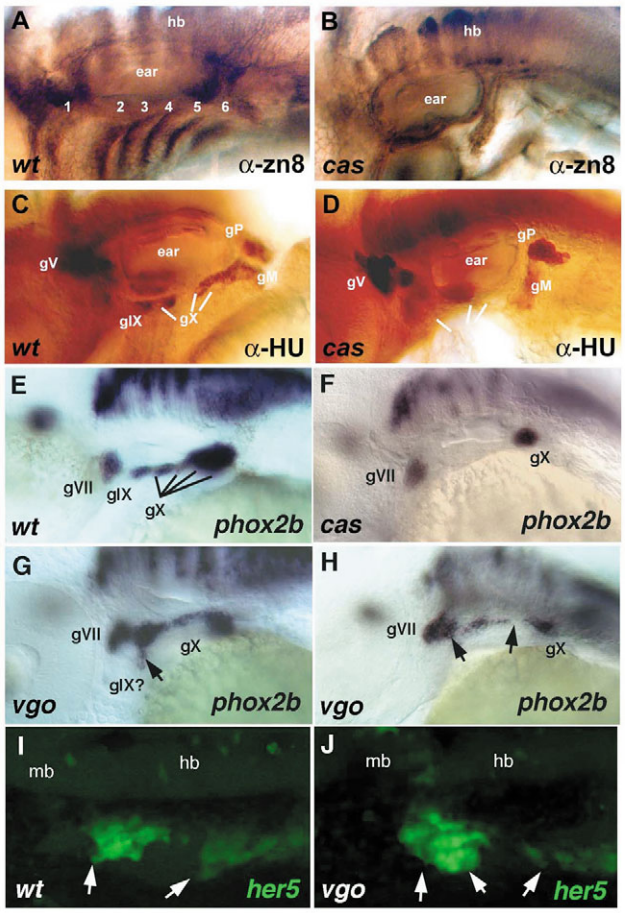

Fig. 3. Epibranchial defects in mutants that disrupt endoderm. Lateral views, anterior to the left. (A,B) Wild type and *cas* mutant at 48 hpf, immunolabeled with anti-zn8 antibody, which labels pharyngeal pouches 1-6. (C,D) Wild type and *cas* mutant at 48 hpf, immunolabeled with anti-Hu to mark sensory neurons. (E,F) Wild type and *cas* mutant at 48 hpf labeled by whole-mount in situ hybridization for *phox2b* mRNA in neural progenitors. (G,H) Examples of *phox2b* expression in *vgo* mutants. Arrow in G denotes a ventrally extended ganglion; arrows in H denote fused or missing ganglia. (I,J) *her5:egfp* expression in living wild type and *vgo* mutant at 24 hpf. Arrows in I denote contacts between pouches and ectoderm; arrows in J denote deformed or missing pouches. 1-5, pharyngeal pouches; gM, medial portion of vagal; gP, posterior lateral line; gV, trigeminal; gIX, glossopharyngeal; gX, vagal; hb, hindbrain; mb, midbrain.

mutants also lacked any expression of *neurod* or *phox2b* in these ganglia (Fig. 3E,F). By contrast, neurons derived from dorsolateral placodes, including the trigeminal (gV) and posterior lateral line (gP) ganglia, as well as the proximal portion of the vagal (gX), appeared to be unaffected in *cas* mutants, and some additional scattered Hu-immunoreactive cells were detected ventral to gP (Fig. 3D). To determine whether earlier placodal specification is disrupted in *cas* mutants, we analyzed expression of *foxi1*, which marks the placodal field during somitogenesis (Fig. 6) (Lee et al., 2003; Nissen et al., 2003; Solomon et al., 2003). No defects were detected in embryos derived from $cas^{+/-}$ heterozygotes at 20 hpf (Fig. 6A,B; n=50), but, by 48 hpf, *foxi1* expression was no longer detected in either the epibranchials or in the pouches in $cas^{-/-}$ mutants (Fig. 6C,D). These results suggest that endoderm is required specifically for neurogenesis in epibranchial, and not dorsolateral, placodes.

In contrast to *cas*, *vgo* mutants form endoderm but their pouches are severely disorganized. Mutants often lack posterior pouches or they appear to fuse along the AP axis, but no defects in cranial ganglia have been reported (Piotrowski and Nusslein-Volhard, 2000). Our analysis of *phox2b* expression, however, revealed consistent defects in epibranchial ganglia in *vgo* (Fig. 3G,H). Subsets of ganglia were missing or fused along the AP axis in many mutants (92%, n=26), and these defects were not always symmetrical on the left and right sides of the pharynx, similar to the variable pouch deformities in mutants. Surprisingly, in many *vgo* mutants the ganglia appeared to be enlarged, and extended further ventrally than in wild-type siblings (Fig. 3G,H). To correlate pouch and placodal defects more directly, we analyzed *vgo* mutants carrying the *her5:egfp* transgene and raised them individually for analysis of *phox2b* expression. Consistent with our analyses in wild type at 24 hpf (Fig. 3I), we found a close correlation between enlarged or reduced contacts made by pouches with the ectoderm and epibranchial defects observed in *vgo* (Fig. 3J). Mutant embryos in which a pouch failed to make this contact showed specific loss of the adjacent ganglion, while in other cases pouches appeared to form larger regions of contact, and these invariably correlated with the presence of more *phox2b*+ neurons (100%, n=14). This further supports the idea of a contact-dependent signal from the lateral, pouch-forming endoderm that controls the spatial extent of neurogenesis in the overlying ectoderm.

Restoration of endoderm rescues cranial ganglia in *cas* mutants

Wild-type cells can form endoderm when transplanted into a *cas* mutant, because *cas* acts downstream of Nodal signaling (Aoki et al., 2002a; Aoki et al., 2002b). Using this approach, we tested whether the reintroduction of endoderm into *cas* mutants was sufficient to restore epibranchial formation. Cells transplanted into the blastula margin in zebrafish contribute to the mesodermal layer, but rarely to the endoderm. However, we can drive cells into the endoderm and rescue the formation of pouches by injecting the donors with an activated form of the Nodal receptor TaramA (tar*) (David et al., 2002). Injections of *cas* mRNA itself also drives donor cells to the endoderm, demonstrating that this is not simply due to the presence of tar* (Fig. 4B). *cas* or tar* RNA was co-injected into wild-type donor embryos together with rhodamine and biotin-conjugated dextrans (10,000 M_r; Molecular Probes) as lineage tracers at the 1-cell stage, and cells were transplanted at early blastula stages into host embryos derived from two $cas^{+/-}$ heterozygotes (Fig. 4A). We then analyzed *phox2b* and *neurod* expression at 40 hpf and compared it with the locations of grafted cells. Transplants of this type form clones of endoderm in various positions, including the pouches (Fig. 4 C-E). Injection of *cas* or tar* alone caused no defects in epibranchial ganglia (Fig. 4B; Fig. 7A).

Grafting of *cas*- or tar*-injected wild-type cells into *cas* mutant hosts efficiently restored *phox2b* (and *neurod*) expression in epibranchial placodes wherever endodermal cells formed pouches (Fig. 4C-E; 100%; n=29; Table 1). No rescue was observed when transplanted cells were located medially in the endoderm or outside of the pharynx. Confocal imaging of

several grafts, revealed a close correlation between the organized movements of endodermal cells into pouches and the locations of *phox2b*+ cells, further suggesting that pouch formation in these mosaics is crucial for rescue. These results demonstrate that the restoration of endodermal pharyngeal pouches in *cas* mutant embryos rescues epibranchial development.

BMP signaling is required locally in endoderm for epibranchial neurogenesis

BMP7 has been shown to induce *Phox2b* expression in chick explants of pharyngeal ectoderm (Begbie et al., 1999) but it is not known: (1) whether BMP signaling is required for this process in vivo; or (2) whether BMPs expressed in endoderm control the spatial localization of placodal neurogenesis. In order to address these issues, we first examined the expression patterns of several zebrafish relatives of BMP7 in the pharyngeal pouches, including *bmp2a*, *bmp2b*, *bmp4* and *bmp7*. All but *bmp7* show expression in the pouches during the stages of epibranchial placode formation. At 22 hpf, *bmp2a*, *bmp2b* and *bmp4* are expressed in the lateral pouches, near the junction between the endoderm and placodal ectoderm (Fig. 5A-C). By 30-40 hpf, *bmp2a* and *bmp2b* are expressed throughout the pouches, whereas *bmp4* remains more distally restricted near the epibranchials (Fig. 5E-G).

In addition, we identified a zebrafish *bmp5* gene that has not been described previously and that is also expressed in the pouches (Fig. 5D,H). Amino acid identities of mature *bmp5* are 84% to mouse and human *BMP5*, 67% to zebrafish *bmp7*, 74% to human *BMP7*, 54% to zebrafish *bmp4*, and 52% to *bmp2a* and *bmp2b*. Furthermore, *bmp5* is not expressed during gastrula or early segmentation stages, unlike its close zebrafish relatives *bmp2b* and *bmp7*, which are required for early dorsoventral patterning. Expression is first detected in sensory patches within the otic placode, and in the pharyngeal region at 22 and 30 hpf (Fig. 5D,H). Pharyngeal expression of *bmp5* includes both arch mesenchyme and pharyngeal pouches, with expression becoming restricted to the dorsal- and ventral-most pouches by 30-40 hpf (Fig. 5H,L).

Consistent with their endodermal defects, expression of all four BMP family members is reduced in *cas* mutants by 40 hpf (Fig. 5I-P). Expression is still present but the pattern is variably disorganized in *vgo* mutants (data not shown). Thus, several BMPs are expressed in the pouches at the appropriate place and time to influence epibranchial neurogenesis, and loss of expression correlates with epibranchial defects in mutants.

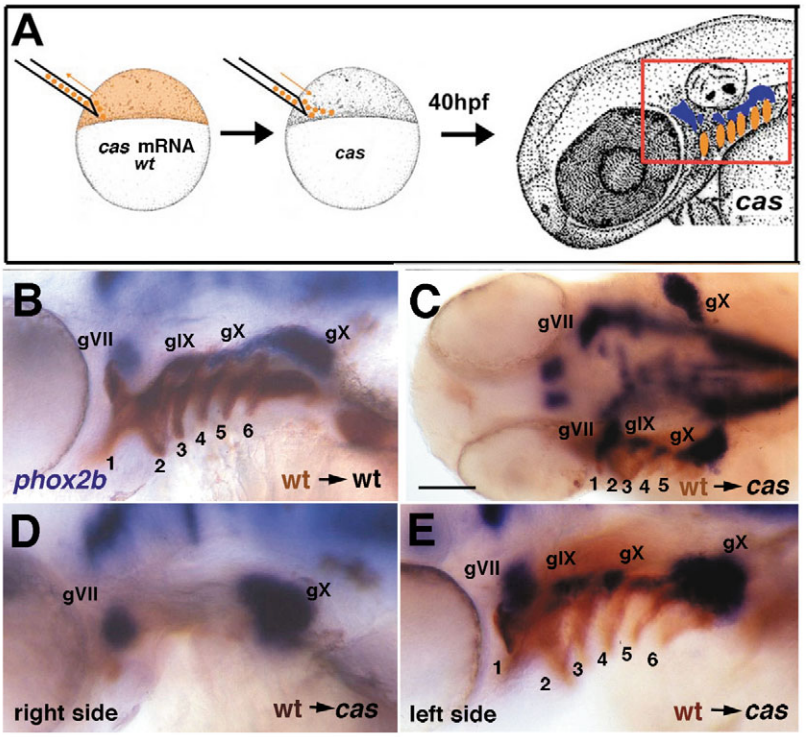

Fig. 4. Restoration of endoderm rescues epibranchial ganglia in *cas/sox32* mutants. (A) Diagram showing transplantation technique. Cells were grafted at blastula stages from *cas* mRNA-injected (or TaramA-injected,tar*), wild-type (wt) donors co-injected with biotinylated-dextran (orange) into unlabeled *cas* mutant hosts. Transplants gave rise to endodermal cells in the arches (box outlined in red) and induced epibranchial ganglia (blue). (B,D,E) Lateral views, 48 hpf, showing examples of epibranchial rescue by such cas-injected endodermal transplants (brown), as determined by in situ hybridization for *phox2b* expression (blue). pf, pectoral fin. (C) Dorsal view. Scale bar: 50 μm.

As Bmp7 plays a role in epibranchial formation in the chick, we examined epibranchials in the *bmp7* zebrafish mutant *snailhouse* (*snh*) (Dick et al., 2000). Analysis of *foxi1* at 20 hpf revealed variable reductions or loss of the early placodal field and pouches (Fig. 6E,F). By 48 hpf, *snh* mutants displayed a severe reduction in epibranchial neurons as determined by the expression of *neurod* (Fig. 6G,H). However *snh* mutants have severe defects in DV patterning and gastrulation that may secondarily cause these defects in neurogenesis.

Therefore, to test more local requirements for BMPs in epibranchial development, we blocked BMP signaling focally in the endoderm by co-injecting *cas* or tar* mRNA and mRNA encoding the *Xenopus* form of the BMP inhibitor *noggin* (*nog*)

Table 1. Reduction of BMP signaling interferes with endoderm-mediated induction of epibranchials

	Transplants (genotype of host embryo)									
Ganglia	*cas* (wt)	*cas* (*cas*)	tar* (wt)	tar* (*cas*)	*cas*/tar* +*nog* (wt)	*cas*/tar* +*nog* (*cas*)	*cas*/tar* +2bMO (wt)	*cas*/tar* +2bMO (*cas*)	*cas*/tar* +2b/5MO (wt)	*cas*/tar* +2b/5MO (*cas*)
Normal	38	5	24	3	23	0	12	0	10	0
Reduced	0	8	0	11	17	2	0	9	16	0
Absent	0	0	0	2	0	19	0	4	0	19

Host embryos were injected with either 500 pg *nog* mRNA, 300 pg *bmp2b*-MO (2bMO) alone or 2bMO together with 1 ng *bmp5*-MO (5MO).

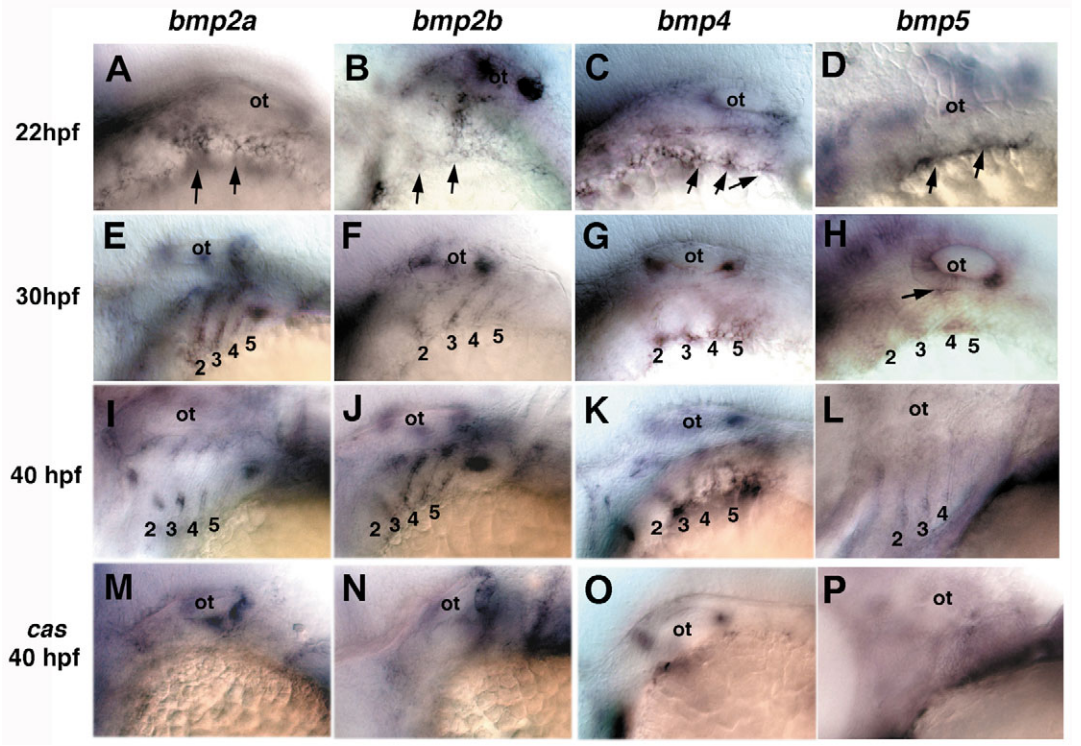

Fig. 5. BMP gene expression in the pharyngeal pouches during epibranchial development, and defects in *cas* mutants. Lateral views, anterior to the left. Whole-mount in situ hybridization was performed in wild types at 22 hpf (top row), 30 hpf (second row) and 40 hpf (third row), and in *cas* mutants at 40 hpf (bottom row), for *bmp2a* (A,E,I,M), *bmp2b* (B,F,J,N), *bmp4* (C,G,K,O) and *bmp5* (D,H,L,P). Arrows indicate initial expression at the ventrolateral edges of each pouch. Arrow in H denotes *bmp5* expression in the dorsal pouches. 1-5, pharyngeal pouches; ot, otic capsule.

(Smith and Harland, 1992), into wild-type donors and transplanting these cells into either wild-type or *cas* mutant hosts. As a control for activity, we showed that injection of 500 pg of *nog* mRNA at the one-cell stage was capable of dorsalizing zebrafish embryos, and we used similar or slightly lower amounts for co-injection with *cas* or tar* (hereafter referred to as *cas*/*nog* or tar*/*nog*). Such *nog*-injected transplanted cells contributed to pharyngeal pouches in equal numbers to cells injected with *cas* or tar* alone, and were generally located on only one side of the pharynx, leaving the contralateral side as an internal control (see Fig. 4). We found that cells co-expressing *cas*/*nog* or tar*/*nog* caused reductions in the number of *phox2b*-expressing cells in adjacent epibranchial ganglia on the same side in wild-type hosts at 48 hpf (37%, n=26; Fig. 7B-D; Table 1). Furthermore, similar transplants into *cas* mutants were completely unable to rescue epibranchial development, even when pharyngeal pouches were clearly restored on the transplanted side (93%, n=15; Fig. 7H,I; Table 1). These results indicate that BMP signaling is required locally to specify the locations of epibranchial placodes, and further suggest that the crucial source of the signal is the endoderm.

To address which specific BMPs are required in epibranchial induction, we used a similar approach, but in this case donors were injected with antisense morpholino oligonucleotides (MOs) to disrupt the expression of zebrafish *bmp2a*, *bmp2b*, *bmp4*, *bmp5* and *bmp7*, either individually or in combination. All of these except for zebrafish *bmp7* are expressed in the

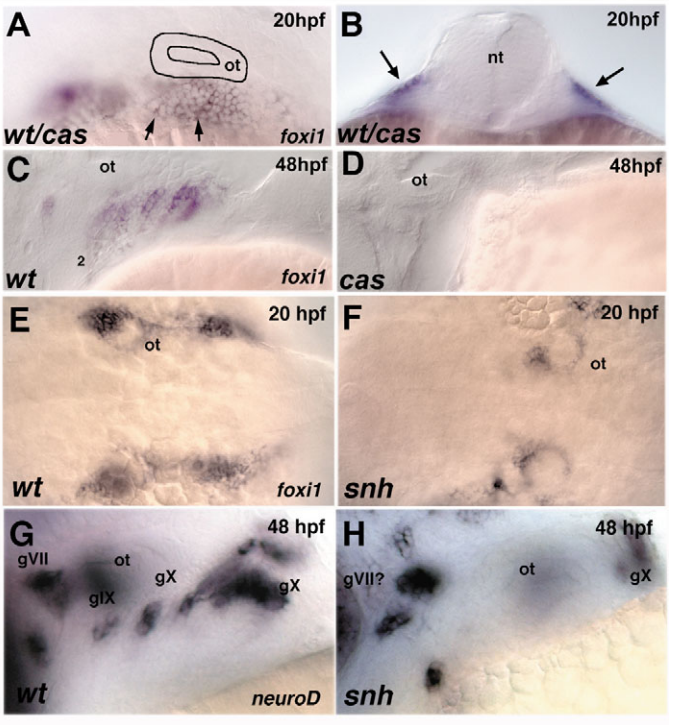

Fig. 6. Early placodal defects in *cas*/*sox32* and *snh*/*bmp7* mutants. Lateral views, anterior to the left except for in B, which is a transverse section, and E,F, which are dorsal views. (A,B) Whole-mount in situ hybridization for *foxi1* in embryos at 20 hpf from a cross between *cas*$^{+/-}$ heterozygotes reveals no difference between wild types and mutants. Arrows in B indicate ectodermal expression. (C,D) *foxi1* expression at 48 hpf in both pouch endoderm and epibranchial placodes in wild type, and loss of expression in cas mutants. (E,F) Dorsal views showing *foxi1* expression at 20 hpf in wild type and severe reduction of expression in *snh*/*bmp7* mutants. (G,H) Lateral views showing *neurod* expression in epibranchial ganglia and severe reductions in *snh*/*bmp7* mutants. 1-6, pharyngeal pouches; gVII, facial; gIX, glossopharyngeal; gX, vagal; nt, neural tube; ot, otic vesicle.

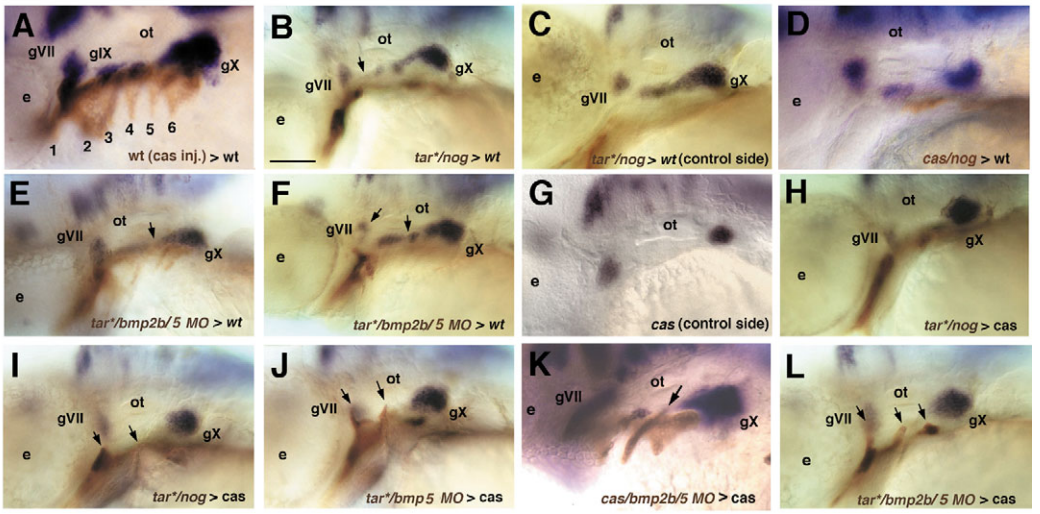

Fig. 7. BMP signaling is required locally in endoderm for epibranchial neurogenesis. Lateral views, anterior to the left. In situ hybridization for *phox2b* mRNA labels epibranchials at 48 hpf in all panels, whereas biotinylated-dextran injected into the donor labels transplanted cells (brown). (A) Wild-type pattern of *phox2b* expression in a control embryo that received a large graft of *cas*-injected endodermal cells. Similar results were obtained with tar*. (B-F) Wild-type hosts that received transplants of donor cells co-injected with tar*/dextran and either *nog* mRNA (B-D) or *bmp2b* and *bmp5* MOs (E,F), which disrupt epibranchial formation (arrows). (G) *phox2b* expression in a *cas* mutant showing lack of epibranchials at 48 hpf. (H-L) Transplantation of tar*/*nog* (H,I) tar*/*bmp5*MO (J), *cas/bmp2b/5*MO-injected (K) or tar*/*bmp2b/5*MO-injected (L) endodermal pouches (arrows) fails to rescue epibranchials in *cas* mutants. Scale bar: 50 μm.

pouches during epibranchial induction (see Fig. 5). We co-injected morpholinos together with *cas* or tar* RNA to create endodermal donors lacking the functions of individual BMPs or combinations thereof (hereafter referred to as *cas*/*bmp*-MO or tar*/*bmp*-MO). To control for morpholino effectiveness, we injected amounts into the donors that produce a complete loss-of-function phenotype for the *bmp2b*-MO (300 pg per embryo phenocopies the *swirl* mutant) (Imai and Talbot, 2001) and *bmp7*-MO (800 pg per embryo phenocopies the *snailhouse* mutant) (Imai and Talbot, 2001). Only the combination of both *bmp2b*- and *bmp5*-MOs into donors consistently caused reductions in epibranchials adjacent to transplanted pouches in wild-type hosts (62%, *n*=26; Fig. 6E,F; Table 1) and completely eliminated the ability of these cells to rescue epibranchials in *cas* mutants (*n*=19, Fig. 7K,L; Table 1). *cas* or tar* mRNA + *bmp2b*-MO or *bmp5*-MO alone slightly reduced the ability of transplanted endodermal cells to rescue epibranchial development in *cas* mutant hosts (64% rescued; *n*=13; Fig. 7J), and had no effect when transplanted into wild types (Table 1). Finally, *cas* or tar* mRNA + *bmp2a*-, *bmp4*- or *bmp7*-MOs had little to no effect on epibranchial development (data not shown). These results suggest that *bmp2b* and *bmp5* are both required within the endoderm for epibranchial induction. Based on their overlapping patterns of expression, these two BMP genes may function redundantly with one another, as well as with *bmp2a* and *bmp4*.

BMPs are both necessary and sufficient to induce epibranchials

To target the stage at which epibranchial induction occurs more precisely, we implanted beads coated with recombinant human BMP or NOG proteins, and assayed the pattern of *phox2b* expression in neural progenitors (Fig. 8). Beads approximately 70-100 μm in diameter, soaked in either 1 μg or 10 μg/ml BMP4 (similar results were obtained with 100 μg/ml BMP5 and BMP7), were placed anterior to the otic vesicle on one side of the head at 20 hpf, embryos were then raised to 48 hpf for *phox2b* analysis by in situ hybridization. Control embryos that received beads soaked in BSA-PBS showed no changes in the pattern of *phox2b* expression (Fig. 8B). By contrast, embryos that received beads soaked in 10 μg/ml BMP4 showed ectopic *phox2b*+ neural progenitors in the vicinity of the bead (53%; *n*=29; Fig. 8C; Table 2), whereas beads soaked in 1 μg/ml

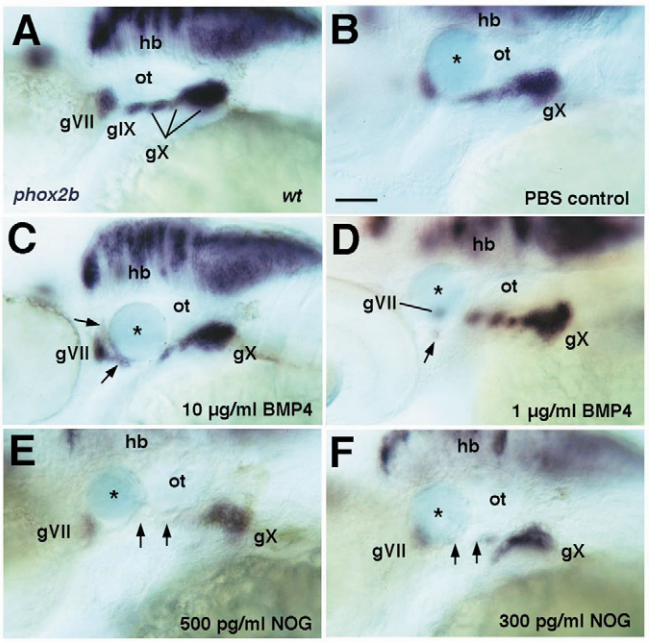

Fig. 8. BMP4-coated beads induce, and NOG-coated beads inhibit, epibranchial formation. Lateral views, anterior to the left. In situ hybridization for *phox2b* mRNA to label epibranchials at 48 hpf. (A) Wild-type control embryo. (B-F) Embryos that received Affi-Gel Blue beads soaked in either PBS (B), BMP4 (10 μg/ml, C; 1 μg/ml, D) or NOG protein (500 pg/ml, E; 300 pg/ml, F). Arrows in C and D indicate ectopic *phox2b*+ cells adjacent to the bead; arrows in E and F denote missing ganglia adjacent to the NOG-coated bead. Asterisks indicate beads. gVII, facial; gIX, glossopharyngeal; gX, vagal; ot, otic vesicle. Scale bar: 50 μm.

Table 2. BMP4- or NOG-coated beads disrupt epibranchials

	Beads implantations				
Ganglia	DMSO	BMP4 (1 μg/μl)	BMP4 (10 μg/μl)	Noggin (100 μg/μl)	Noggin (500 μg/μl)
Ectopic	0	5	15	0	0
No defect	24	28	9	3	1
Reduced	0	3	5	7	8
Absent	0	0	0	0	3

BMP4 produced a much weaker effect (8%; *n*=36; Fig. 8D; Table 2). This effect was very local, occurring only when beads were placed in the branchial region, and ectopic epibranchial induction did not spread into ectoderm outside of the arches. Conversely, beads soaked in 500 μg/ml recombinant NOG and implanted into this region consistently showed a reduction in epibranchials on the implanted side (92%, *n*=12; Fig. 8E,F; Table 2). A slightly weaker effect was observed with beads soaked in 100 μg/ml NOG (70%; *n*=10; Fig. 8D; Table 2). These results suggest that at 20 hpf, as pharyngeal pouches are beginning to contact the surface, pharyngeal ectoderm is competent to respond to BMPs and form neurons. They also show that BMP signaling is required within the pharyngeal region at this stage for epibranchial induction.

Discussion

In this study, we have shown that signals from the endoderm in zebrafish are essential for induction of the epibranchial subdivision of the peripheral nervous system, and that BMPs are one component of this signaling. Epibranchial ganglia develop as ectodermal placodes adjacent to each of the pharyngeal pouches, serially reiterated outgrowths of the endodermal wall of the pharynx that are the first morphological signs of pharyngeal segmentation (Goodrich, 1930). Our experiments suggest that contact between a pouch and the adjacent ectoderm is essential to specify the locations of these placodes and to promote neurogenesis, and that the induction in zebrafish is mediated in part by *bmp2b* and *bmp5* (Fig. 9). Little is known about the signals that induce the formation of other primary sensory neurons in vertebrates, but these may involve similar interactions.

Endodermal pouches specify the locations of ectodermal placodes

Several lines of evidence support this hypothesis. First, each pharyngeal pouch contacts the ectoderm within an hour or two of the onset of neurogenic gene expression in the adjacent placode. Second, endodermal defects in *cas* or *vgo* mutants correlate with placodal defects. Third, endodermal grafts locally rescue neurogenic gene expression in epibranchial placodes in *cas*, demonstrating that the loss of placodes in this mutant is due to loss of endoderm and not defects in neural crest cells or other cell types in the vicinity of the epibranchials. This promotion of epibranchial development by underlying endodermal pouches serves to coordinate the pattern of cranial ganglia with the pharyngeal arches that they innervate.

Our results support those of Begbie et al. (Begbie et al., 1999), who performed explant studies in chick and showed that *Phox2b*+ neural progenitors form in ectodermal explants when co-cultured with endoderm in collagen gels. From these studies, however, it remained unclear whether such interactions occur in vivo, or are necessary for neurogenesis. We have used genetic ablation and reintroduction of endoderm in zebrafish to demonstrate an in vivo requirement. Whether or not this induction is direct, or requires an intermediate signal via neighboring tissues remains unclear. However, the close spatial proximity between pharyngeal pouches and epibranchial placodes within an arch, as well as the coincidence between early epibranchial defects in *cas* and *vgo* mutants, supports the idea of a direct signal (Fig. 9). Because these endodermal mutants only show defects in epibranchial and not dorsolateral placodes, our results also support the model proposing that these two groups of sensory neurons are induced by different signals (Graham and Begbie, 2000). This would also help to explain the presence of additional placodes associated with the ventral regions of the pouches in some species, such as the hypobranchial ganglia in *Xenopus* (Schlosser, 2003).

To visualize this interaction between the pouches and placodes, we followed the expression of *her5:egfp* in the pharyngeal endoderm in living embryos (Tallafuss and Bally-Cuif, 2003). Confocal time-lapse analysis of *her5:egfp* expression revealed dramatic and rapid changes in endodermal cell shape during pouch morphogenesis. Lateral endodermal cells of the pharynx align mediolaterally to form pouches and

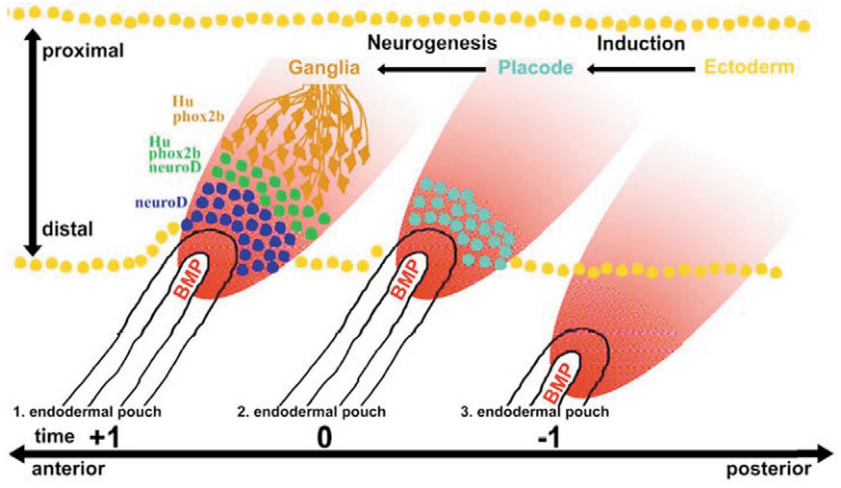

Fig. 9. Model for epibranchial induction and neurogenesis. Diagram indicating the sequence of placodal specification and neurogenesis within a ganglion, and its induction by an endodermal pouch. Maturation occurs in an anterior to posterior sequence as surface ectoderm becomes specified as placodal tissue that then undergoes neurogenesis. Newly born *neurod*+ cells (blue) form distally in response to BMPs from a pouch as it contacts the surface. These are then displaced proximally to become neuroblasts (green) that also express *phox2b* and Hu. They then differentiate, stop expressing *neurod* (orange) and extend axons toward the hindbrain. gAD, dorsal anterior lateral line; gAV, ventral anterior lateral line; gP, posterior lateral line; gV, trigeminal; gVII, facial (geniculate); gVIII, auditory; gIX, glossopharyngeal (petrosal); gX, vagal (nodose); ot, otic placode; tg, trigeminal.

extend filopodia toward the surface, eventually contacting the overlying ectoderm. This contact occurs at almost exactly the same stage at which we could detect the first signs of epibranchial neurogenesis, with contact occurring a few hours prior to the onset of *neurod* expression in most cases. These results further reinforce the idea that pouches regulate both the spatial and temporal formation of neural progenitors in the placodes. Consistent with this hypothesis, we show that ectopic epibranchials in *vgo* mutants are associated with abnormal extensions of pouches (Piotrowski and Nusslein-Volhard, 2000). In addition, ectopic *neurod* expression was induced by endodermal transplants into *cas* mutants that formed ectopic contacts with the ectoderm. These results indicate that a broader region of pharyngeal ectoderm is competent to form placodal neurons, but only does so in response to endoderm.

Epibranchial neurogenesis: neural crest versus placodes

Many cranial sensory ganglia have a dual embryonic origin from both neural crest and placodes, in contrast to those of the trunk, which are purely crest derived. Crest cells form the proximal epibranchial ganglia in chick, whereas placodally derived cells lie further distally, and the proportions of these differ in each ganglion (Ayer LeLievre and LeDouarin, 1982; D'Amico-Martel and Noden, 1983; Webb and Noden, 1993). Placodally derived neurons differentiate early and establish the first peripheral and central axonal projections of the sensory nerves. Epibranchial neurons also are displaced inwards along neural crest migratory pathways as they mature, and require the crest to establish their appropriate innervation in the hindbrain (Begbie and Graham, 2001). Our analyses of gene expression within the epibranchial ganglia in zebrafish confirm that there is a similar proximodistal sequence of neurogenesis within the placodally derived neurons in zebrafish, in which newborn *neurod*+ neurons form adjacent to the pharyngeal pouch and older *phox2b* and Hu+ neurons lie further proximally (Fig. 8).

Both *cas* and *vgo* mutants disrupt distal neurogenesis in the vagal ganglion complex (gX_{1-4}), but retain a more proximal population of neural progenitors that develops independently of endodermal influences. These may be the neural crest-derived equivalent in fish of the proximal nodose ganglion (gX) in chick. Consistent with this hypothesis, proximal gX is less affected than other epibranchial ganglia in *Ngn2*$^{-/-}$ (Fode et al., 1998) and *Phox2a*$^{-/-}$ (Morin et al., 1997) mutant mice, as well as in *foxi1*$^{-/-}$ mutant zebrafish (Lee et al., 2003). Future cell tracing studies are necessary to determine which portions of these ganglia are derived from neural crest in zebrafish, but our previous lineage studies suggest that at least some of the proximal neurons are crest derived (Schilling and Kimmel, 1994). Our results suggest that these proximal epibranchial neurons are BMP-independent or, alternatively, may be induced by BMPs from other sources, such as the otic vesicle.

BMP signals are both necessary and sufficient for placode specification

We also show a requirement for BMP signaling in the control of epibranchial neurogenesis, and specifically implicate *bmp2b* and *bmp5* in this process in zebrafish. This is based on several lines of evidence: (1) *bmp2b* and *bmp5* are expressed in the pouches as they form; (2) targeted knockdown of *bmp2b* and *bmp5* expression with morpholinos specifically in the endoderm locally disrupts placode induction; and (3) the BMP inhibitor NOGGIN locally disrupts epibranchial ganglia while misexpression of BMP proteins using beads induces ectopic neurons. Begbie et al. (Begbie et al., 1999) showed that *Bmp7* in the chick is expressed in the pharyngeal endoderm and that recombinant BMP7 protein was sufficient to induce neurogenesis in ectodermal explants. They also found that Follistatin blocks the induction of neurogenesis by endoderm in these cultures, further indicating a role for TGFβ signaling in this process. Our results are the first to demonstrate a specific requirement for BMP signaling in vivo, and suggest that multiple members of this family, including *bmp2b* and *bmp5*, are essential.

Bmp4 (a close relative of *bmp2b*) and *Bmp7* have been implicated in many aspects of neurogenesis and peripheral nervous system (PNS) development. For example, they mediate interactions between the neural plate and epidermal ectoderm that induce neural crest cells, as well as secondary sensory neurons within the spinal cord (Liem et al., 1995). Later, the same two BMPs are secreted by the dorsal aorta and promote a subset of adjacent neural crest cells to express *Phox2a* and to form sympathetic neurons (Reissmann et al., 1996). Yet, *Bmp4*$^{-/-}$ mutant mice die prior to PNS formation and no PNS defects have been described in *Bmp7*$^{-/-}$ mutants. Our results may help to explain this apparent discrepancy by showing that at least two BMPs, *bmp2b* and *bmp5*, are partially redundant for this process.

Other signaling molecules have been implicated in neurogenic placode induction, and it is important to understand how their functions relate to those of BMPs. Foremost among these are the FGFs. For example, signals from the MHB (possibly FGF8) are thought to induce the trigeminal (gV), a dorsolateral placode that we have shown does not require endodermal BMP signals in zebrafish. FGF3 and FGF8 produced in the hindbrain are involved in induction of the otic placode (Phillips et al., 2001), which also develops independently of endoderm. Both *fgf3* and *fgf8* are expressed in both the pharyngeal endoderm and ectoderm, and potentially act together with BMPs in epibranchial induction (David et al., 2002; Crump et al., 2004b). However, in the chick *Fgf8* is only expressed in a ventral, posterior domain within each pouch, which abuts the domain of *Bmp7* and is not in contact with the placode (Graham and Begbie, 2000), suggesting that *Fgf8* and *Bmp7* interact to define territories of expression within the endoderm. Recent evidence in zebrafish has implicated *fgf3* in epibranchial development (D. Raible, personal communication). Thus, it will be interesting to determine whether Fgfs act synergistically with BMPs in this interaction, or if different growth factors give qualitatively different responses in placodal cells. BMP2 and FGF act synergistically to induce neuronal differentiation of PC12 cells (Hayashi et al., 2001). The augmentation of FGF-induced differentiation by BMP2 occurs through the upregulation of FGFR1 several hours after BMP2 expression (Hayashi et al., 2003). Similarly, BMPs might also commit epibranchial progenitor cells to neuronal differentiation induced by FGFs. The combined actions of different growth factors may underlie differences not only between types of placode (e.g. FGF in dorsolaterals, BMP in epibranchials), but also in the specification of the distinct

types of neurons that form in each ganglion within a class (Vogel and Davies, 1993).

A central role for the endoderm in patterning head segments

Segmentation of the foregut into pouches is a fundamental feature of the head and there is growing evidence that this plays a crucial patterning role. The segmental characteristics of the pharyngeal pouches develop independently of the presence of neural crest cells (Veitch et al., 1999). Pharyngeal slits are also found in non-vertebrate chordates, such as amphioxus, suggesting that their appearance predated that of placodes or neural crest during evolution. The formation of pouches during embryogenesis coincides with and affects the segmental development of many cell types within the pharyngeal arches, including both neurogenic placodes and neural crest (Begbie et al., 1999; LeDouarin, 1982; David et al., 2002; Couly et al., 2002). Endoderm may provide some guidance cues for neural crest migration; however, most evidence suggests that it plays a more important role later, in local interactions between pouches and immediately adjacent neural or skeletal progenitors, and our results are consistent with this. The size, shape and orientation of neural crest-derived cartilages are prefigured in the shapes of certain pouches, both in fish (Crump et al., 2004a; Crump et al., 2004b) and in chick (Couly et al., 2002). Likewise, we have shown that the location and size of epibranchial sensory ganglia are prefigured by contacts between pouches and the surface ectoderm. Defects in these endoderm-dependent processes appear to underlie human craniofacial malformations such as DiGeorge syndrome (often caused by mutations in TBX1), and our results would suggest that some cranial sensory nerve deficits in humans might also reflect defects in endoderm. Our studies establish a genetic context in zebrafish in which to now examine how these signals control sensory neurogenesis.

We thank I. Blitz for the *Xenopus noggin* expression construct. We also thank A. Graham, I. Blitz and members of the Schilling Laboratory for critical reading of the manuscript. This work was supported by the NIH (NS-41353, DE-13828), March of Dimes (1-FY01-198) and Pew Scholars Foundation (2615SC) to T.F.S., and a VolkswagenStiftung Junior Research Group Grant to L.B.-C.

References

Andermann, P., Ungos, J. and Raible, D. W. (2002). Neurogenin1 defines zebrafish cranial sensory ganglia precursors. *Dev. Biol.* **251**, 45-58.

Anderson, D. J. (1999). Lineages and transcription factors in the specification of vertebrate primary sensory neurons. *Curr. Opin. Neurol.* **9**, 517-524.

Aoki, T., Mathieu, J., Saint-Etienne, L., Peyreiras, N. and Rosa, F. (2002a). Regulation of Nodal signaling and mesendoderm formation by TARAM-A, a TGFb-related type I receptor. *Dev. Biol.* **241**, 273-288.

Aoki, T. O., David, N. B., Minchiotti, G., Saint-Etienne, L., Dickmeis, T., Persico, G. M., Strahle, U., Mourrain, P. and Rosa, F. M. (2002b). Molecular integration of *casanova* in the Nodal signalling pathway controlling endoderm formation. *Development* **129**, 275-286.

Ayer-LeLievre, C. S. and LeDouarin, N. M. (1982). The early development of cranial sensory ganglia and the potentialities of their component cells studied in quail-chick chimeras. *Dev. Biol.* **94**, 291-310.

Baker, C. V. H. and Bronner-Fraser, M. (2001). Vertebrate cranial placodes. I. Embryonic induction. *Dev. Biol.* **232**, 1-61.

Baker, C. V., Stark, M. R., Marcelle, C. and Bronner-Fraser, M. (1999). Competence, specification and induction of Pax-3 in the trigeminal placode. *Development* **126**, 147-156.

Bally-Cuif, L., Goutel, C., Wassef, M., Wurst, W. and Rosa, F. (2000). Coregulation of anterior and posterior mesendodermal development by a hairy-related transcriptional repressor. *Genes Dev.* **14**, 1664-1677.

Begbie, J. and Graham, A. (2001). Integration between the epibranchial placodes and the hindbrain. *Science* **294**, 595-598.

Begbie, J., Brunet, J. F., Rubenstein, J. and Graham, A. (1999). Induction of the epibranchial placodes. *Development* **126**, 895-902.

Begbie, J., Ballivet, M. and Graham, A. (2002). Early steps in the production of sensory neurons by the neurogenic placodes. *Mol. Cel. Neurosci.* **21**, 502-511.

Buj-Bello, A., Buchman, V. L., Horton, A., Rosenthal, A. and Davies, A. M. (1995). GDNF is an age-specific survival factor for sensory and autonomic neurons. *Neuron* **15**, 821-828.

Couly, G., Creuzet, S., Bennaceur, S., Vincent, C. and Le Douarin, N. M. (2002). Interactions between Hox-negative cephalic neural crest cells and the foregut endoderm in patterning the facial skeleton in the vertebrate head. *Development* **129**, 1061-1073.

Crump, J. G., Swartz, M. E. and Kimmel, C. B. (2004a). An integrin-dependent role of pouch endoderm in hyoid cartilage development. *PloS Biol.* E244.

Crump, J. G., Maves, L., Lawson, N. D., Weinstein, B. M. and Kimmel, C. B. (2004b). An essential role for Fgfs in endodermal pouch formation influences later craniofacial skeletal pattern. *Development* **131**, 5703-5716.

D'Amico-Martel, A. and Noden, D. M. (1983). Contributions of placodal and neural crest cells to avian cranial peripheral ganglia. *Am. J. Anat.* **166**, 445-468.

David, N. B., Saint-Etienne, L., Tsang, M., Schilling, T. F. and Rosa, F. M. (2002). Requirement for endoderm and FGF3 in ventral head skeleton formation. *Development* **129**, 4457-4468.

Dick, A., Hild, M., Bauer, H., Imai, Y., Maifeld, H., Schier, A. F., Talbot, W. S., Bouwmeester, T. and Hammerschmidt, M. (2000). Essential role of Bmp7 (*snailhouse*) and its prodomain in dorsoventral patterning of the zebrafish embryo. *Development* **127**, 343-354.

Dickmeis, T., Mourrain, P., Saint-Etienne, L., Fischer, N., Aanstad, P., Clark, M., Strahle, U. and Rosa, F. (2001). A crucial component of the endoderm formation pathway, CASANOVA, is encoded by a novel sox-related gene. *Genes Dev.* **15**, 1487-1492.

Fode, C., Gradwohl, G., Morin, X., Dierich, A., LeMeur, M., Goridis, C. and Guillemot, F. (1998). The bHLH protein Neurogenin-2 is a determination factor for epibranchial placode-derived sensory neurons. *Neuron* **20**, 483-494.

Goodrich, E. (1930). *Studies on the Structure and Development of Vertebrates.* London: MacMillan (Reprinted in 1958 by Dover Publications, New York and Constable, London).

Graham, A. and Begbie, J. (2000). Neurogenic placodes: a common front. *Trends Neurosci.* **23**, 313-316.

Guo, S., Brush, J., Teraoka, H., Goddard, A., Wilson, S. W., Mullins, M. C. and Rosenthal, A. (1999). Development of noradrenergic neurons in the zebrafish hindbrain requires BMP, FGF8, and the homeodomain protein soulless/Phox2a. *Neuron* **24**, 555-566.

Hall, B. K. (1980). Tissue interactions and the initiation of osteogenesis and chondrogenesis in the neural crest-derived mandibular skeleton of the embryonic mouse as seen in isolated murine tissues and recombinations of murine and avian tissue. *J. Embryol. Exp. Morphol.* **58**, 251-264.

Hayashi, H., Ishisaki, A., Suzuki, M. and Imamura, T. (2001). BMP-2 augments FGF-induced differentiation of PC12 cells through upregulation of FGF receptor-1 expression. *J. Cell Sci.* **114**, 1387-1395.

Hayashi, H., Ishisaki, A. and Imamura, T. (2003). Smad mediates BMP-2-induced upregulation of FGF-evoked PC12 cell differentiation. *FEBS Lett.* **536**, 30-34.

Imai, Y. and Talbot, W. S. (2002). Morpholino phenocopies of the bmp2b/*swirl* and bmp7/*snailhouse* mutations. *Genesis* **30**, 160-163.

Kikuchi, Y., Agathon, A., Alexander, J., Thisse, C., Waldron, S., Yelon, D., Thisse, B. and Stainier, D. Y. (2000). Casanova encodes a novel Sox-related protein necessary and sufficient for early endoderm formation in zebrafish. *Genes Dev.* **15**, 1493-1505.

Kimmel, C. B., Ballard, W. W., Kimmel, S. R., Ullmann, B. and Schilling, T. F. (1995). Stages of embryonic development of the zebrafish. *Dev. Dyn.* **203**, 253-310.

Korzh, V., Sleptsova, I., Liao, J., He, J. and Gong, Z. (1998). Expression of zebrafish bHLH genes ngn1 and nrd defines distinct stages of neural differentiation. *Dev. Dyn.* **213**, 92-104.

Le Douarin, N. M. (1982). *The Neural Crest.* Cambridge, UK: Cambridge University Press.

Lee, S. A., Shen, E. L., Fiser, A., Sali, A. and Guo, S. (2003). The zebrafish

forkhead transcription factor foxi1 specifies epibranchial placode-derived sensory neurons. *Development* **130**, 2669-2679.

Liem, K. F., Tremml, G., Roelink, H. and Jessell, T. M. (1995). Dorsal differentiation of neural plate cells induced by Bmp-mediated signals from the epidermal ectoderm. *Cell* **82**, 969-979.

Luo, G., Hofmann, C., Bronckers, A. L., Sohocki, M., Bradley, A. and Karsenty, G. (1995). Bmp-7 is an inducer of nephrogenesis, and is also required for eye development and skeletal patterning. *Genes Dev.* **9**, 2808-2820.

Ma, Q., Chen, Z., del Barco Barrantes, I., de la Pompa, J. L. and Anderson D. J. (1998). Neurogenin-1 is essential for the determination of neuronal precursors for proximal cranial sensory ganglia. *Neuron* **20**, 469-482.

Martinez-Barbera, J. P., Toresson, H., Da Rocha, S. and Krauss, S. (1997). Cloning and expression of three members of the zebrafish Bmp family, bmp2a, bmp2b and bmp4. *Gene* **198**, 53-59.

Marusich, M. F., Furneaux, H. M., Henion, P. and Weston, J. A. (1994). Hu neuronal proteins are expressed in proliferating neurogenic cells. *J. Neurobiol.* **25**, 143-155.

Morin, X., Cremer, H., Hirsch, M. R., Kapur, R. P., Goridis, C. and Brunet, J. F. (1997). Defects in sensory and autonomic ganglia and absence of locus coeruleus in mice deficient for the homeobox gene Phox2a. *Neuron* **18**, 411-423.

Nissen, R. M., Yan, J., Amsterdam, A., Hopkins, N. and Burgess, S. M. (2003). Zebrafish foxi one modulates cellular response to fgf signaling required for the integrity of ear and jaw patterning. *Development* **130**, 2543-2554.

Phillips, B. T., Bolding, K. and Riley, B. B. (2001). Zebrafish fgf3 and fgf8 encode redundant functions for otic placode formation. *Dev. Biol.* **235**, 351-365.

Piotrowski, T. and Nusslein-Volhard, C. (2000). The endoderm plays an important role in patterning the segmented pharyngeal region in zebrafish (Danio rerio). *Dev. Biol.* **225**, 339-356.

Piotrowski, T., Schilling, T. F., Brand, M., Jiang, Y. J., Heisenberg, C. P., Beuchle, D., Grandel, H., van Eeden, F. J., Furutani-Seiki, M., Granato, M. et al. (1996). Jaw and branchial arch mutants in zebrafish. II. Anterior arches and cartilage differentiation. *Development* **123**, 345-356.

Piotrowski, T., Ahn, D., Schilling, T. F., Nair, S., Ruvinsky, I., Geisler, R., Rauch, G.-J., Haffter, P., Zon, L. I., Zhou, Y. et al. (2003). The zebrafish *van gogh* mutation disrupts tbx1, which is involved in the DiGeorge deletion syndrome in humans. *Development* **130**, 5043-5052.

Reissmann, E., Ernsberger, U., Francis-West, P. H., Brickell, P. D. and Rohrer, H. (1996). Involvement of bone morphogenetic protein-4 and bone morphogenetic protein-7 in the differentiation of the adrenergic phenotype in developing sympathetic neurons. *Development* **122**, 2079-2088.

Schilling, T. F. and Kimmel, C. B. (1994). Segment and cell type lineage restrictions during pharyngeal arch development in the zebrafish embryo. *Development* **120**, 483-494.

Schlosser, G. (2003). Hypobranchial placodes in Xenopus laevis give rise to hypobranchial ganglia, a novel type of cranial ganglia. *Cell Tissue Res.* **312**, 21-29.

Schlosser, G. and Northcutt, R. G. (2000). Development of neurogenic placodes in Xenopus laevis. *J. Comp. Neurol.* **418**, 121-146.

Smith, W. C. and Harland, R. M. (1992). Expression cloning of noggin, a new dorsalizing factor localized to the Spemann organizer in Xenopus embryos. *Cell* **70**, 829-840.

Solomon, K. S., Kudoh, T., Dawid, I. G. and Fritz, A. (2003). Zebrafish foxi1 mediates placode formation and jaw development. *Development* **130**, 929-940.

Sommer, L., Ma, Q. and Anderson, D. J. (1996). Neurogenins, a novel family of atonal-related bHLH transcription factors, are putative mammalian neuronal determination genes that reveal progenitor cell heterogeneity in the developing CNS and PNS. *Mol. Cell. Neurosci.* **8**, 221-241.

Stark, M. R., Sechrist, J., Bronner-Fraser, M. and Marcelle, C. (1997). Neural tube-ectoderm interactions are required for trigeminal placode formation. *Development* **124**, 4287-4295.

Tallafuss, A. and Bally-Cuif, L. (2003). Tracing of her5 progeny in zebrafish transgenics reveals the dynamics of midbrain-hindbrain neurogenesis and maintenance. *Development* **130**, 4307-4323.

Thisse, C., Thisse, B., Schilling, T. F. and Postlethwait, J. H. (1993). Structure of the zebrafish snail gene and its expression in wild-type, spadetail and no tail mutant embryos. *Development* **119**, 1203-1215.

Tiveron, M. C., Hirsch, M. R. and Brunet, J. F. (1996). The expression pattern of the transcription factor Phox2a delineates synaptic pathways of the autonomic nervous system. *J. Neurosci.* **16**, 7649-7660.

Trevarrow, B., Marks, D. L. and Kimmel, C. B. (1990). Organization of hindbrain segments in the zebrafish embryo. *Neuron* **4**, 669-679.

Valarche, I., Tissier-Seta, J., Hirsch, M., Martinez, S., Goridis, C. and Brunet, J. F. (1993). The mouse homeodomain protein Phox2 regulates Ncam promoter activity in concert with Cucx/CDP and is a putative determinant of neurotransmitter phenotype. *Development* **119**, 881-896.

Veitch, E., Begbie, J., Schilling, T. F., Smith, M. M. and Graham, A. (1999). Pharyngeal arch patterning in the absence of neural crest. *Curr. Biol.* **9**, 1481-1484.

Vogel, K. S. and Davies, A. M. (1993). Heterotopic transplantation of presumptive placodal ectoderm changes the fates of sensory neuron precursors. *Development* **119**, 263-276.

Webb, J. F. and Noden, D. M. (1993). Ectodermal placodes: contributions to the development of the vertebrate head. *Amer. Zool.* **33**, 434-447.

Westerfield, M. (1995). *The Zebrafish Book. A Guide for the Laboratory Use of Zebrafish* (Danio rerio), 3rd edn. Eugene, OR: University of Oregon Press.